Hard diffraction from small-size color sources[*]

F. Hautmann

Department of Physics, Pennsylvania State University, University Park PA 16802, USA

Z. Kunszt

Institute of Theoretical Physics, ETH, CH-8093 Zurich, Switzerland

D.E. Soper

Institute of Theoretical Science, University of Oregon, Eugene OR 97403, USA
and Theory Division, CERN, CH-1211 Geneva 23, Switzerland

We describe diffractive hard processes in the framework of QCD factorization and discuss what one can learn from the study of hadronic systems with small transverse size.

Diffractive deeply inelastic structure functions satisfy a factorization theorem of the form [1–3]

$$F_2^{\text{diff}} \sim \hat{F}_a \otimes \frac{df_{a/A}^{\text{diff}}}{dx_P \, dt} \quad , \tag{1}$$

where the first factor on the right hand side is a short-distance scattering function and the second factor is a diffractive parton distribution, containing the long-distance physics. The short distance factor is no different than in inclusive deeply inelastic scattering. The long distance factor is. Although the evolution equation for the diffractive parton distribution functions is the same as that of the inclusive parton distribution functions [1,2,4], their behavior at a fixed scale μ_0 that serves as the starting point for evolution may be very different from the behavior of the inclusive functions. The different phenomenology that characterizes diffractive versus inclusive deeply inelastic scattering depends entirely on this.

Diffractive parton distributions in a proton at the scale μ_0 are not perturbatively calculable. This is because the proton has a large transverse size. Suppose one had a hadron of a size $1/M$ that is small compared to $1/\Lambda_{\text{QCD}}$. Then one could compute diffractive parton distributions as a perturbation expansion. Results on diffraction of small-size hadronic systems have been presented in Ref. [5].

Fig. 1 shows a typical Feynman graph for one such case. Here we have considered a color-singlet current that couples only to heavy quarks of mass $M \gg \Lambda_{\text{QCD}}$. This system gets diffracted and acts as a color source with small radius. This is represented in the lower part of the graph. The top part of the graph represents the bilocal field operator [2] that defines the gluon distribution. The particular Feynman graph in Fig. 1, although of a rather high order in α_s, is leading in the limit $1/x_P \to \infty$, where x_P is the fractional loss of longitudinal momentum from the diffracted hadron.

The physical picture that emerges from the analysis of graphs like that shown in Fig. 1 in the limit $1/x_P \to \infty$ is that of the familiar "aligned jet" model [6]. The bilocal operator creates a large-momentum parton together with a color source of the opposite color. This is confined to move on a lightlike line and is part of the definition of the (inclusive or diffractive) parton distribution functions. This happens far from the incoming small-size hadron. The system created by the operator then passes through the color field of the small-size hadron, absorbing two gluons. What we have, then, is the scattering of two color dipoles.

At this order of perturbation theory, the result for the diffractive parton distributions has the following form

---

[*]Talk given by F. Hautmann at the Division of Particles and Fields Conference, Los Angeles, January 5-9, 1999.
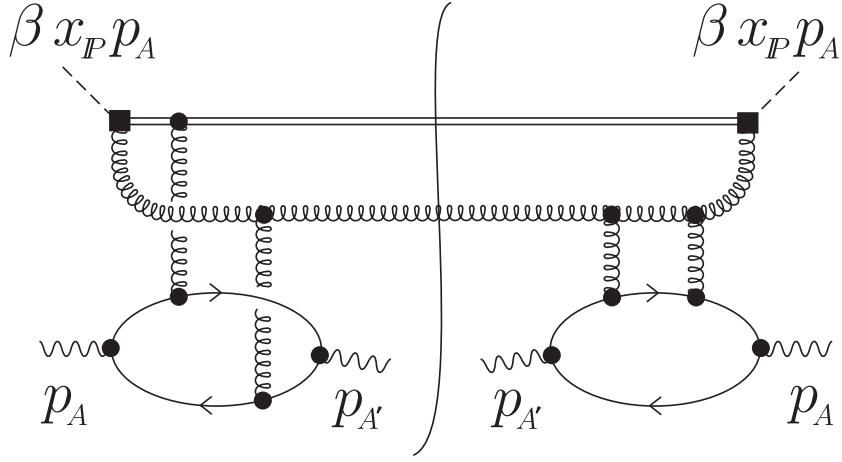
FIG. 1. A typical Feynman graph contributing to the diffractive gluon distribution of the model vector meson.

$$\frac{df_{a/A}^{\mathrm{diff}}}{dx_P\,dt}(\beta, x_P, \mathbf{q}^2, M) = \frac{\alpha^2\,e_Q^4\,\alpha_s^4}{x_P^2\,M^2}\,h_a(\beta, \mathbf{q}^2/M^2)\,[1 + \mathcal{O}(x_P)] \quad . \tag{2}$$

Here βx_P is the fraction of the hadron's longitudinal momentum carried by the parton and $\mathbf{q}$ is the diffracted transverse momentum ($t \approx -\mathbf{q}^2$). The functions h_a are plotted in Fig. 2.
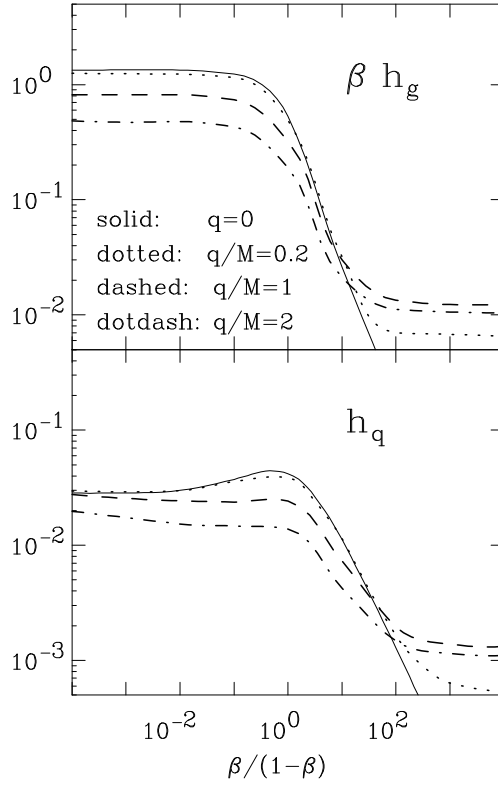

FIG. 2. The β dependence of the gluon (above) and quark (below) diffractive distributions for different values of $\mathbf{q}^2 \simeq |t|$. The rescaled distributions h_a are defined in Eq. (2).

For small β the distributions behave as

$$h_g \propto \beta^{-1} , \quad h_q \propto \beta^0 \quad (\beta \to 0) . \tag{3}$$

For large β, both the gluon and quark distributions evaluated at any finite $\mathbf{q}$ have a constant behavior:

$$h_g, h_q \propto (1-\beta)^0 \quad (\beta \to 1, \ \mathbf{q} \neq 0) . \tag{4}$$

At $\mathbf{q} = 0$ there are cancellations in the leading $\beta \to 1$ coefficients, so that the distributions vanish in the $\beta \to 1$ limit:

$$h_g \propto (1-\beta)^2 , \quad h_q \propto (1-\beta)^1 \quad (\beta \to 1, \ \mathbf{q} = 0) . \tag{5}$$

The distributions are dominated by small $|t| \simeq \mathbf{q}^2$ everywhere except at very large β. Note that

$$h_g \gg h_q . \tag{6}$$

Roughly, the order of magnitude of the ratio between the diffractive gluon and quark distributions can be accounted for by the ratio of the associated color factors, $C_A^2 \, (N_c^2 - 1)/[C_F^2 \, N_c] = 27/2$.

The result given above does not describe scaling violation. When additional gluons are emitted from the top subgraph in Fig. 1, on the other hand, ultraviolet divergences arise. The renormalization of these divergences leads to the dependence of the diffractive parton distributions on a renormalization scale μ. This dependence is governed by the renormalization group evolution equations. The higher order, ultraviolet divergent graphs are suppressed compared to the graphs of the type in Fig. 1 by a factor $\alpha_s \log(\mu^2/M^2)$. When $\log(\mu^2/M^2)$ is large, these contributions are important, and thus evolution is important. On the other hand, when μ is of the same order as the heavy quark mass M, the higher order contributions are small corrections to the graphs considered above. Thus one may interpret the result given above as a result for the diffractive parton distributions at a fixed scale of order $\mu^2 \approx M^2$. Then the diffractive parton distributions at higher values of μ^2 are given by solving the evolution equations with the result of Eq. (2) as a boundary condition.

How are these calculations for small-size systems related to the real world? Obviously, the protons probed in deeply inelastic scattering experiments at HERA have a large transverse size. Suppose that one had available a hadron of adjustable size. Start with a very small size, in which case diffraction is forced to take place mostly on short distances, and let the size increase. Since this scale acts as a physical infrared cut-off, longer and longer distances are now allowed to contribute to the diffraction process. In a naive perturbation expansion, by the time one gets to 1 fm (about the proton radius) the answer would be completely dominated by the soft region. On the other hand, as the size of the hadronic system increases, nonperturbative dynamics sets in. The infrared-sensitive behavior suggested by the perturbative power counting is likely smoothed out by this dynamics. We hypothesize that, as we go to larger and larger sizes, the distance scales that dominate the diffraction process, rather than continuing to grow, stay frozen at some intermediate, semihard scale. The effect of this is to enhance the contribution from hard physics with respect to the contribution from soft physics.

Note that recent experimental observations on the x_P dependence in diffraction may be regarded as providing support for the hypothesis of dominance of semihard scales in the diffractive parton distributions. It has been stressed [7] that the value of $\alpha_P(0) - 1$ (where $\alpha_P(0)$ is the pomeron intercept) measured in diffractive deeply inelastic scattering [8,9] differs by a factor of 2 from the corresponding value measured in soft hadron-hadron cross sections.

We may explore this hypothesis by investigating whether the short-distance result that we have found for small-size systems is also relevant to describe the physics of diffraction from large-size objects, such as protons at HERA. In particular, we are interested in two features of the HERA data for F_2^{diff} [8,9]: the surprising delay in the fall-off with Q^2 and the surprising flatness in β.

To carry out this study, we set M in Eq. (2) equal to $1.5 \, \text{GeV}$ and take the scale dependence of the diffractive parton distributions to be that given by the two-loop evolution equations with the results (2) as a boundary condition at $\mu = M$. The choice of the value for M corresponds to choosing a value for the semihard scale discussed above.

3

The value of this scale, strictly speaking, is to be regarded as a free parameter to be adjusted phenomenologically. In setting the value to $1.5\,\mathrm{GeV}$ we are guided by the expectation that this scale should be roughly of the order of a GeV. See below for some qualitative remarks on different choices.

The upper panel of Fig. 3 shows the result we obtain for the scale dependence of the diffractive (flavor-singlet) quark distribution at a fixed value of β, $\beta = 0.2$. (In this figure the dependence on $\mathbf{q}^2 \simeq |t|$ is integrated over, from 0 to M^2). By comparison, in the lower panel we show the analogous result for the ordinary (inclusive) quark distribution, taken from the standard set CTEQ4M [10]. Fig. 3 illustrates the different pattern of scaling violation in diffractive and inclusive deeply inelastic scattering. At moderate values of momentum fractions, while the ordinary quark distribution is flat or weakly decreasing with Q^2, the diffractive distribution is rising with Q^2. The explanation for the rise in the diffractive case lies with the behavior of the distributions at the initial scale M (Fig. 2). More precisely, it depends on the gluon distribution being dominant throughout the range of momentum fractions. As Q^2 increases, gluons splitting into $q\bar{q}$ pairs feed the quark distribution and cause it to grow in the region of moderately large β.
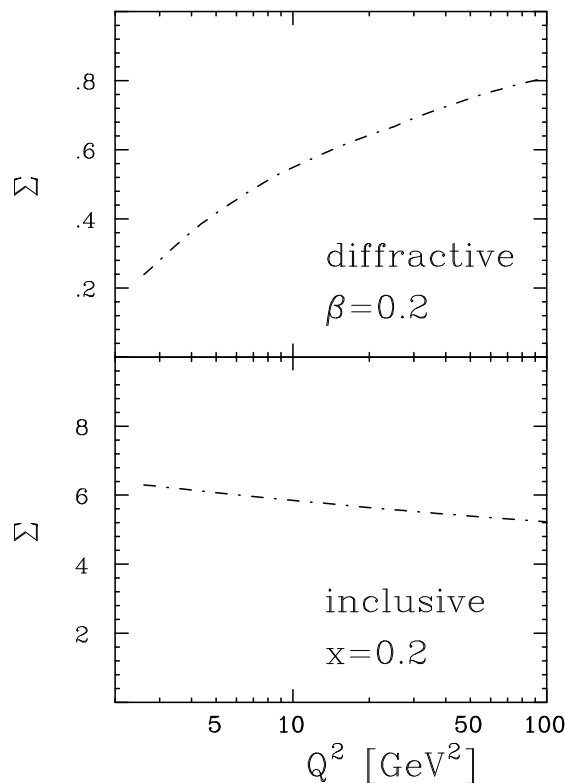

FIG. 3.   Scaling violation in the (flavor-singlet) quark distribution Σ at moderate values of momentum fractions. Above is the case of the diffractive distribution, below is the case of the inclusive distribution (from the set CTEQ4M).

In Fig. 4 we show results for the diffractive structure function F_2^{diff} as functions of β at various values of Q^2. In Fig. 5 we show the same results along with the ZEUS data [9]. Notice the main qualitative features of these results. The sign of the scaling violation is positive up to about $\beta \approx 0.55$, reflecting the behavior noted for the quark distribution Σ in Fig. 3. In the range of intermediate values of β (centered about $\beta \approx 0.5$) F_2^{diff} is rather flat in β. These features are distinctive of the diffractive structure function compared to the inclusive structure function.

These features are in qualitative agreement with what is seen in the HERA data (Fig. 5). Note that, once one combines the analysis of diffraction from small-size states with the hypothesis of dominance of semihard scales (with a particular scale choice), all the dependences of the structure function are fully determined. That is, not only the

Q^2 dependence but also the β dependence are determined from theory. (The same applies to the t dependence. In
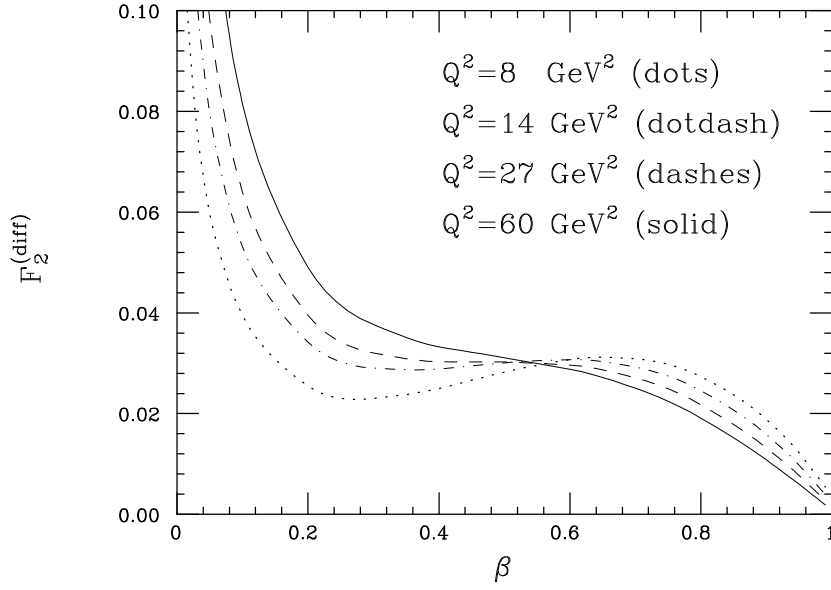

FIG. 4.   The β dependence of the diffractive structure function F_2^{diff} for different values of Q^2. We compute F_2^{diff} in next-to-leading order.
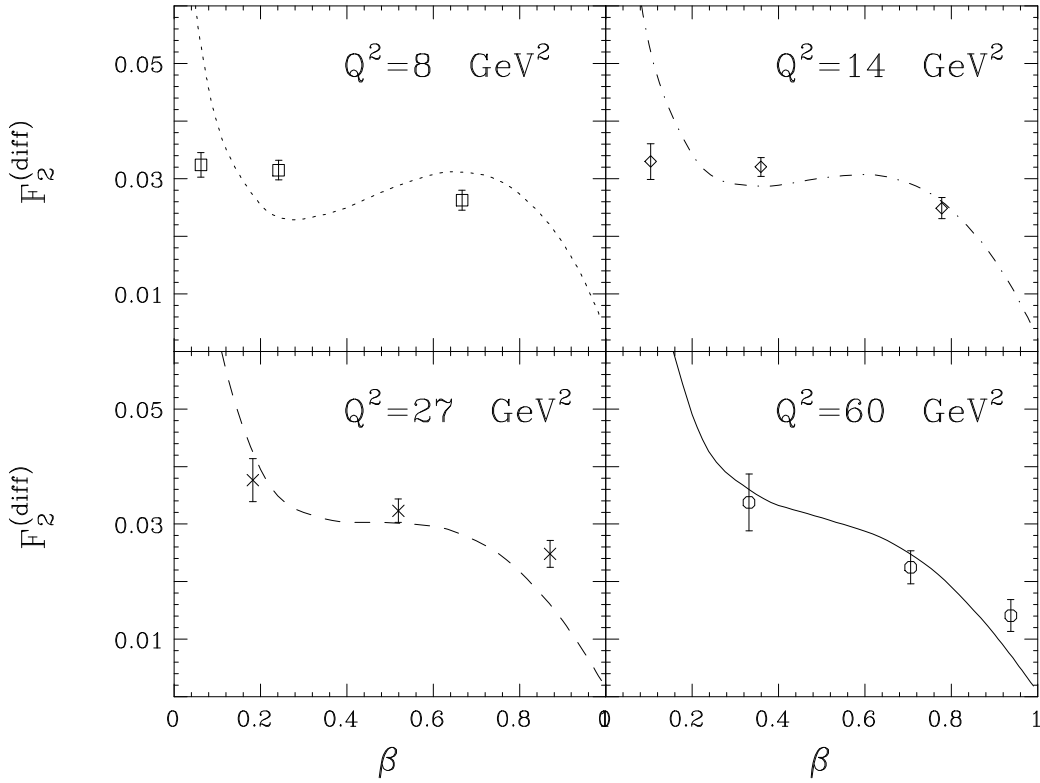

FIG. 5.   Same as in Fig. 4. Also shown are the ZEUS data from Ref. [9].

the results presented here t is integrated over.) The only free parameter left is an overall normalization, which has been adjusted arbitrarily in Figs. 4,5.

In the region of small β, the curves of Figs. 4,5 have a different behavior from that suggested by the two data points at the lowest values of β and lowest values of Q^2 ($Q^2 = 8\,\mathrm{GeV}^2$ and $Q^2 = 14\,\mathrm{GeV}^2$). If further data were to confirm this difference, this could point to interesting effects. Here we limit ourselves to a few qualitative remarks. As far as the theoretical curves are concerned, we note that the diffractive distributions that serve as a starting point for the evolution are fairly mild as $\beta \to 0$. The gluon distribution goes like $1/\beta$, while the quark distribution goes like a constant (see Eq. (3)). The small-β rise of the structure function F_2^{diff} in the curves of Figs. 4,5 is essentially due to the form of the perturbative evolution kernels. As regards the data, it has been observed [11] that for small β the experimental identification of the rapidity gap signal may be complicated by the presence of low $p_\perp$ particles in the final state. If the current data hold up and especially if the same features are observed at lower values of β, it would be interesting to see whether detailed models for the saturation of the unitarity bound [12] could accommodate this small β behavior.

It is of interest to study how the comparison in Fig. 5 changes as the value of the semihard scale M is changed. For example, one may be interested to lower this scale with respect to the value of $1.5\,\mathrm{GeV}$ used so far. For $M = 1\,\mathrm{GeV}$ we find that, roughly speaking, the overall description of the data is of comparable quality (except at the lowest β and Q^2 values, where the discrepancy noted above becomes more pronounced). However, we also find, in particular from the modest steepness of the β shape at the highest Q^2, that a scale a bit higher than $1\,\mathrm{GeV}$ seems to be preferred, perhaps suggesting that the pomeron is a relatively "small" object. We do not push this study to a quantitative level at present, but it appears that in the future more and better data on diffraction could be able to give us useful information on the value of this scale. It would be very interesting if one could connect it to other nonperturbative scales that enter in related areas of hadronic physics.

[1] J.C. Collins, Phys. Rev. D **57**, 3051 (1998).

[2] A. Berera and D.E. Soper, Phys. Rev. D **53**, 6162 (1996).

[3] L. Trentadue and G. Veneziano, Phys. Lett. B **323**, 201 (1994).

[4] T. Gehrmann and W.J. Stirling, Z. Phys. C **70**, 89 (1996); K. Golec-Biernat and J. Kwiecinski, Phys. Lett. B **353**, 329 (1995); Z. Kunszt and W.J. Stirling, in *Proceedings of the International Workshop on Deep Inelastic Scattering DIS96*, Rome, Italy, 1996, edited by G. D'Agostini and A. Nigro (World Scientific, Singapore, 1997), p.240; L. Alvero, J.C. Collins, J. Terron and J. Whitmore, Phys. Rev. D **59**, 074022 (1999).

[5] F. Hautmann, Z. Kunszt and D.E. Soper, Phys. Rev. Lett. **81**, 3333 (1998); Pennsylvania State preprint PSU-TH/207 (1999), to appear.

[6] J.D. Bjorken, AIP Conference Proceedings No. 6, Particles and Fields subseries No. 2, edited by M. Bander, G. Shaw and D. Wong (AIP, New York, 1972); J.D. Bjorken and J. Kogut, Phys. Rev. D **8**, 1341 (1973); J.D. Bjorken, J. Kogut and D.E. Soper, Phys. Rev. D **3**, 1382 (1971); J.D. Bjorken, preprint SLAC-PUB-7096 (1996), hep-ph/9601363.

[7] A.H. Mueller, in *Proceedings of the International Workshop on Deep Inelastic Scattering DIS98*, Brussels, Belgium, April 1998.

[8] H1 Collaboration, (C. Adloff *et al.*), Z. Phys. C **76**, 613 (1997); ZEUS Collaboration (J. Breitweg *et al.*), Eur. Phys. J. C**1**, 81 (1998).

[9] ZEUS Collaboration (J. Breitweg *et al.*), Eur. Phys. J. C**6**, 43 (1999).

[10] H.L. Lai et al., Phys. Rev. D **55**, 1280 (1997).

[11] J. Ellis and G.G. Ross, Phys. Lett. B **384**, 293 (1996); J. Ellis, G.G. Ross and J. Williams, hep-ph/9812385.

[12] E. Gotsman, E. Levin and U. Maor, Nucl. Phys. **B493**, 354 (1997); J. Jalilian-Marian, A. Kovner, A. Leonidov and H. Weigert, Phys. Rev. D **59**, 034007 (1999); K. Golec-Biernat and M. Wüsthoff, hep-ph/9903358.